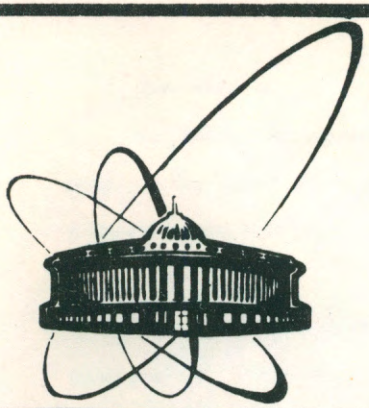

объединенный
институт
ядерных
исследований
дубна



E17-89-281

W.Salejda*

# THE VIBRATIONAL SPECTRA OF THE ONE-DIMENSIONAL FIBONACCI-TYPE QUASICRYSTALS

Submitted to "Acta Physica Polonica"

* On leave of absence from Institute of Physics,
Technical University of Wroclaw,
Wybrzeze Wyspianskiego 27,
50-370 Wroclaw, Poland

1989

1. Introduction

Following the experimental discovery of the icosahedral phase in the aluminium-manganese alloy by Schechtman et al. [1], much attention has been focused on the systems called aperiodic crystals [2-20].

Levine and Steinhardt [ 3,4 ] have introduced the notion of quasiperiodic crystals or quasicrystals (QC) for short. There are three distinguishing features in the definition of QC: (1) The ideal QC exhibit a long-range quasiperiodic positional order (i.e. the mass density function is quasiperiodic or almost periodic ); (2) They have long-range orientational order ( the bond angles between neighbouring atoms are oriented ( on the average ) along an arbitrary chosen set of star axes) ; (3) They are the special kind of Delaunay systems [21] ( the separation l between nearest-neighbouring sites in quasilattice obeys the relations $0 < r < l < R < \infty$ ).

The one-dimensional quasicrystal (1D QC) is defined by the positions $R_n$ of its atoms [4] given (in dimensionless form) by

$$R_n = n + \alpha + \frac{1}{\rho}\left[\frac{n}{\sigma} + \beta\right], \qquad (1)$$

where $\alpha$ , $\beta$ , $\rho$ and $\tau$ are the real numbers, [y] denotes the integer part of y and n is an integer number.

If $\rho=\sigma=\tau$, where $\tau$ is the golden ratio equal to $(1+\sqrt{5})/2$, then, (1) defines the one-dimensional Fibonacci quasicrystal (1D FQC) [4,5].

The spacing $d_{n+1,n}$ between any two neighbour atoms can be expressed as

$$d_{n+1,n} = 1 + \frac{1}{\tau}\left(\left[\frac{n+1}{\tau}+\beta\right] - \left[\frac{n}{\tau}+\beta\right]\right) =$$

$$= \begin{cases} 1 & \text{if } \left[\frac{n+1}{\tau}+\beta\right] = \left[\frac{n}{\tau}+\beta\right] \\ 1+\frac{1}{\tau} & \text{if } \left[\frac{n+1}{\tau}+\beta\right] \neq \left[\frac{n}{\tau}+\beta\right] \end{cases} \qquad (2).$$

The binary quasiperiodic sequence (BQS) $\{d_{n+1,n}\}$ defines the positional long-range order in 1D FQC ( notice that the two distances 1 and $1+1/\tau$ are neither periodically nor randomly spaced).

The electronic and phononic properties of the one-dimensional quasicrystals are studied currently in the framework of simple models [22-41] .

The purpose of this paper is to investigate within the proposed harmonic model the properties of vibrational spectra (VS) of 1D FQC's.

The considered model describes the lattice dynamics of periodic and Fibonacci chain of atoms. The parameter $q = z / \tau$, $z > 0$, called the parameter of quasiperiodicity (POQ), measures deviation of a model from the ideal, periodic one corresponding to $q= z=0$.

Unlike the previous investigations [ 32-41], the next-nearest-neighbour interactions are taken into consideration.

The detailed numerical studies of the structure and fractal dimension of VS are performed in a wide range of model parameter using the free end boundary conditions (FEBC).

The paper is organized as follows. The specification of the model in Sec.2 is given. In Sec.3 the eigenvalue problem for



dynamical matrix (DM) is described. The used numerical methods and results of computer simulations are presented in Sec.4. Sec.5 contains main conclusions and Sec.6 is the summary.

## 2. Harmonic model

We consider a chain of N atoms the equilibrium positions of which are given by (1). The lattice dynamics of 1D FQC is defined by the Hamiltonian

$$H_{ph} = \sum_{l=1}^{N} \frac{P_l^2}{2 M_l} + \frac{1}{2}\sum_{l=1}^{N} k_{l,l+1}\,(u_l - u_{l+1})^2 + \frac{1}{2}\sum_{l=1}^{N} g_{l,l+2}\,(u_l - u_{l+2})^2 , \qquad (3)$$

where $P_l$ and $u_l$ are the momentum and the displacement of the l-th atom, respectively, $M_l$ denotes the mass of the l-th atom, $k_{l,l+1}$ and $g_{l,l+2}$ are the force constants of nearest-neighbour (NN) and next-nearest-neighbour (NNN) interactions , respectively.

Within the harmonic Hamiltonian (3) we can model the lattice dynamics of 1D FQC in two ways [42] : we can define the BQS describing dependences of force constants $\{k_{l,l+1}\}$ and $\{g_{l,l+2}\}$ on atom distances $d_{l,l+1}$ and $d_{l,l+2}$ or we can specify the BQS describing the atom masses $\{M_l\}$ , respectively.

In this paper we use the first approach [ 32,33,35 ]. We assume that $M_l = m_o$ for all l and the magnitudes of the force constants describing NN and NNN interactions of the l-th atom are ( see Fig.1)

$$k_{l+1,l} = k_o \{ 1 + q (1 - [(l+1)/\tau] - [l/\tau]) \} \quad (4)$$

$$g_{l+2,l} = g_o \{ 1 + q (2 - [(l+2)/\tau] - [l/\tau]) \} , \quad (5)$$

where $q=z/\tau$ is POQ; $k_o$ and $g_o$ denote spring constants.

Hamiltonian (3) and BQSs given by (4) and (5) define harmonic model vibrational spectra of which we will study numerically.

We point out that for $z > 0$ and $z = 0$ equations (3-5) describe the Fibonacci-type and periodic chain of atoms, respectively.

BQSs (4) and (5) take two values (see Fig.1)

$$k_{l+1,l} = \begin{cases} k_o(1+q) & \text{if } d_{l+1,l} = 1 \\ k_o & \text{if } d_{l+1,l} = 1 + 1/\tau \end{cases} \quad (4a)$$

$$g_{l+2,l} = \begin{cases} g_o(1+q) & \text{if } d_{l+2,l} = 2 + 1/\tau \\ g_o & \text{if } d_{l+2,l} = 2 + 2/\tau \end{cases} \quad (5a).$$

Note that the mathematical properties of infinite BQSs generated by

$$r(\mu,\nu,l)=[(l+1)/\mu+\nu]-[l/\mu+\nu] \quad l=1,2,\ldots,N , \quad (6)$$

where $\nu$ and $\mu>1$ are real irrational numbers have been recently studied by Aviram [43,44]. Using the results of Refs. 43,44 in Appendix A some mathematical properties of BQSs (4) and (5) are given .

## 3. Eigenvalue problem

Equations of motion have the form



$$m_o \ddot{u}_l = k_{l,l-1}( u_{l-1} - u_l ) + k_{l,l+1}( u_{l+1} - u_l ) + g_{l,l-2}( u_{l-2} - u_l ) + g_{l,l+2}( u_{l+2} - u_l ) \quad (7)$$

$$l=1,2,\ldots,N .$$

We introduce new mass dependent variables $u_l = Q_l \sqrt{m}$ and we shall seek the normal stationary modes of lattice vibrations in the form [ 45 ]

$$Q_l(t) = Q_l^o \exp(i \omega_o t) . \quad (8).$$

Substituting (8) into (7) we obtain

$$\Omega^2 Q_l = \alpha_l Q_l + \beta_{l-1} Q_{l-1} + \beta_{l+1} Q_{l+1} + \gamma_{l-2} Q_{l-2} + \gamma_{l+2} Q_{l+2} \quad (9)$$

$$l=1,2,\ldots,N ,$$

where the following dimensionless variables have been used

$$\alpha_l = 2 ( 1 + q ) - q \left( \left[ \frac{l+1}{\tau} \right] - \left[ \frac{l-1}{\tau} \right] \right) + h \left( 2 ( 1 + 2 q ) - q \left( \left[ \frac{l+2}{\tau} \right] - \left[ \frac{l-2}{\tau} \right] \right) \right) \quad (10)$$

$$-\beta_{l+1} = 1 + q - q \left( \left[ \frac{l+1}{\tau} \right] - \left[ \frac{l}{\tau} \right] \right) \quad (11)$$

$$-\gamma_{l+2} = h \left( 1 + 2 q - q \left( \left[ \frac{l+2}{\tau} \right] - \left[ \frac{l}{\tau} \right] \right) \right) \quad (12)$$

and $\Omega^2 = m_o \omega_o^2 / k_o$; $h = g_o / f_o$ defines the strength of NNN interaction.

Notice that $\beta_{l+1} = - k_{l+1,l} / k_o$ , $\gamma_{l+2} = - h\ g_{l+2,l} / g_o$ and $\alpha_l = - ( \beta_l + \beta_{l+1} + \gamma_l + \gamma_{l+2} )$. For a given N average numbers

$N_{-1}$ and $N_{-1-q}$ of (-1) and -(1+q) in sequence (11) are given by $[N/\tau]$ and $[(1-1/\tau)N]$, respectively. Since (12) is a successor of (11) ( see property A4 in Appendix A ) average numbers $N_{-h(1+q)}$ and $N_{-h}$ of -h(1+q) and -h terms in (12) are $[2\tau N/(2\tau+1)]$ and $[N/(2\tau+1)]$, respectively. Sequence (10) takes three values: $\alpha^{(1)}= 2\ (1+h\ (\ 1+q\ ))$, $\alpha^{(2)}=(\ 1+h\ )(\ 2+q\ )$, $\alpha^{(3)}=2+\ q\ +\ 2\ h\ (\ 1+q\ )$. Therefore, in (10) there are on average $[N/\tau^3]$, $[N/\tau^3]$ and $[N(1-2/\tau^3)]$ of $\alpha^{(1)}$, $\alpha^{(2)}$ and $\alpha^{(3)}$ terms, respectively.

From Eqs. (9) it follows that the frequencies of normal vibrations of 1D FQC are the eigenvalues of N*N symmetrix band matrix of width five if FEBC are applied ( i.e. $k_{1,0} = k_{N,N+1} = g_{1,-1} = g_{2,0} = g_{N+1,N-1} = g_{N+2,N} = 0$ ). In this case (11) and (12) give the off-diagonal elements of DM for $2 \le l \le N$ and $3 \le l \le N$, respectively; $\beta_1=\gamma_1=\gamma_2=0$. (10) define values of $\alpha_l$ for $3 \le l \le N-2$ and $\alpha_1 = -\beta_2 - \gamma_3$ , $\alpha_2 = -\beta_2 -\beta_3 - \gamma_4$ ,$\alpha_{N-1}= -\beta_{N-1}-\beta_N - \gamma_{N-1}$. $\alpha_N= -\beta_N - \gamma_N$.

## 4. Numerical results

In order to study the influence of model parameters on the properties of VS, the G(x) and ΔG(x) functions for $N=10^5$ and various values of q and h are calculated . The integrated density of states (IDOS) G(x), determines the number of eigenfrequencies $\Omega_i$ of DM fulfilling the condition $\Omega_i^2 < x$ . The function ΔG(x) is a histogram of G(x),i.e. $\Delta G(x)= G(x) - G(x-\Delta)$ where Δ is an elementary step of calculations. Notice that x denotes a square of dimensionless eigenfrequency $x=\Omega^2= m_o\omega_o^2/k_o$.



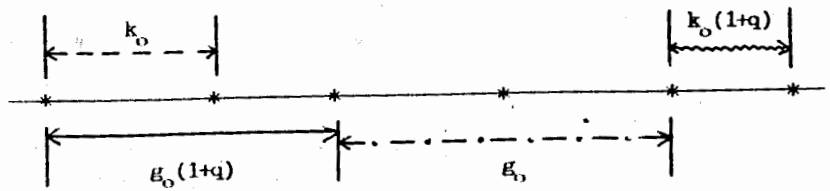


Fig.1. The model of harmonic interactions in 1D FQC; $k_o(1+q)$ (←——→), $k_o$ (←– – –→) and $g_o(1+q)$ (←——→), $g_o$ (←–·–·–→) are the force constants of interactions between nearest-neighbour and next-nearest-neighbour atoms, respectively.

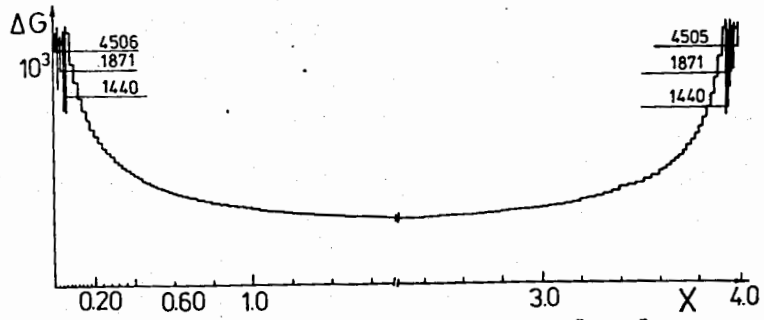


Fig.2. The histogram ΔG(x) as a function of $x=\Omega^2=m_o\omega^2/k_o$; z=0 (i.e.an ideal periodic chain),h=0.0,$N=10^5$,an elementary step of calculation $\Delta=2*10^{-2}$. In the acoustic and optical region values of ΔG are given.

IDOS is calculated using Dean's [45] method. The explicit form of the numerical algorithm is as follows. We calculate a sequence of scalars { $u_l$ } given by

$$u_1=\alpha_1 - x \qquad (13a)$$

$$u_2=\alpha_2 - x - \beta_2^2/u_1 \qquad (13b)$$

$$u_j=\alpha_j - x - \gamma_j^2/u_{j-2} - (\beta_j - \beta_{j-1}\gamma_j/u_{j-2})^2/u_{j-1} \qquad j \ge 3\ , \qquad (13c)$$

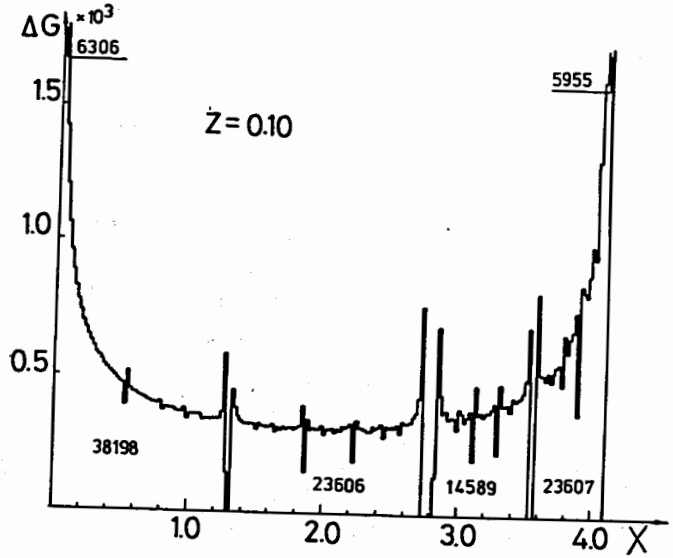


Fig.3a. The same as in Fig.2 for $q=0.1/\tau$ ; $h=0, \Delta=0.02$; numbers depicted inside subbands give the number of eigenstates.

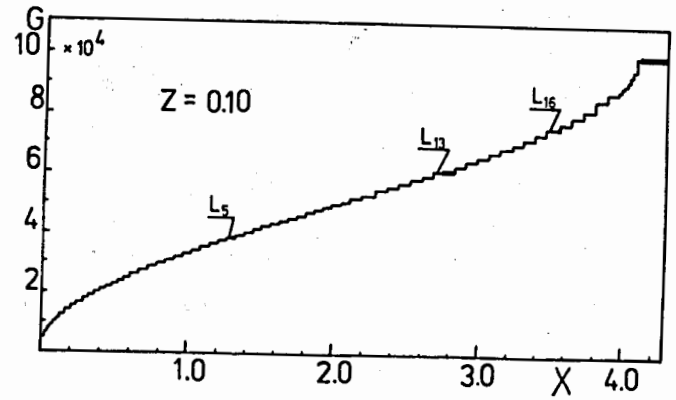


Fig.3b. G(x) as a function of dimensionless square of eigenfrequency $x=\Omega^2=m_0\omega_0^2/k_0$ for $q=0.1/\tau$ , $h=0$ ; $L_i$ denote the values of G(x) at the corresponding x (see Table 1). The bold horizontal lines represent the gaps in the spectrum.



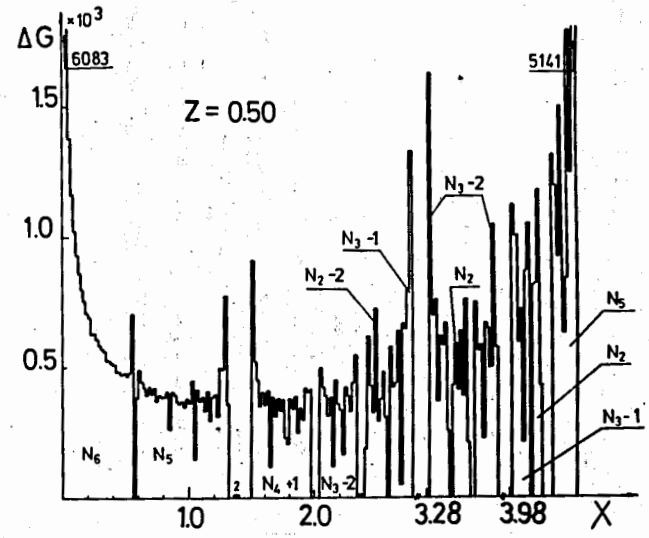


Fig.4a. The same as in Fig.2 for $q=0.5/\tau$ . $N_i$ denote the number of states in subbands (see Table 2).

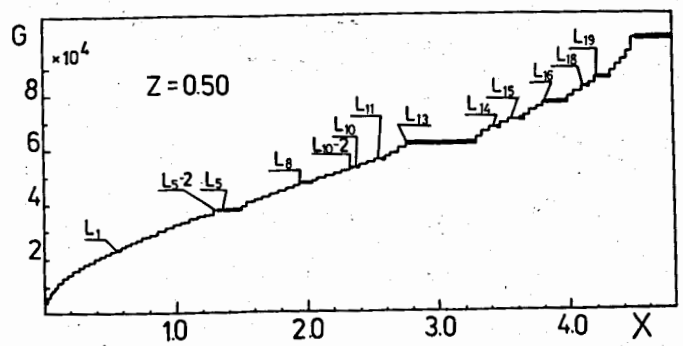


Fig.4b. The same as in Fig.3b for $q=0.5/\tau$ .

where x is a real number and $\alpha_j, \beta_j, \gamma_j$ are the matrix elements of DM. G(x) is found from the signs of n scalar quantities $\{u_i\}$, i.e.

$$G(x) = N_{\{u_i\}}(x), \qquad (14)$$

where $N_{\{u_i\}}(x)$ denotes the numbers of negative $u_i$'-s in the sequence (13).

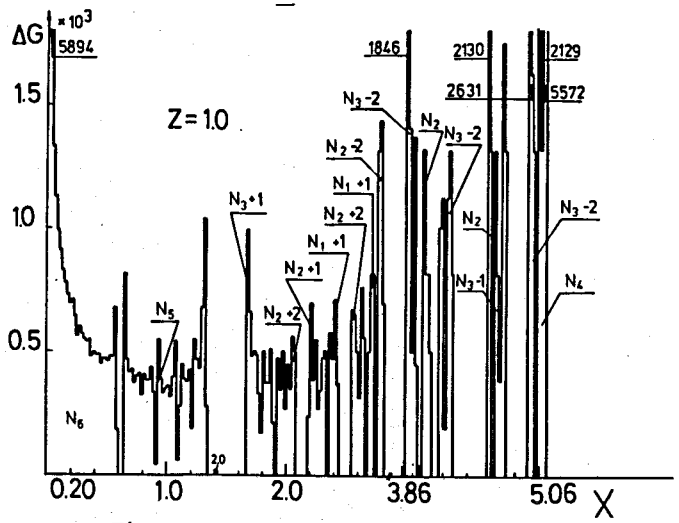


Fig.5a. The same as in Fig.2 for $q=1/\tau$.

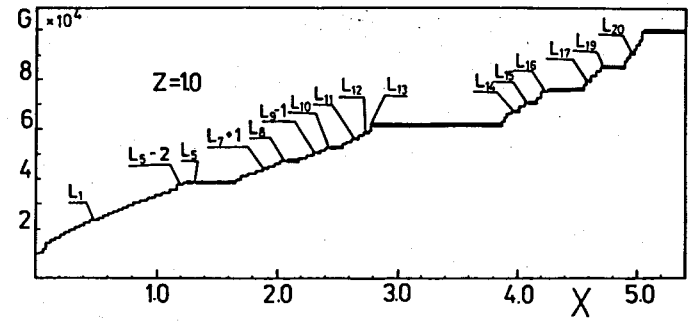


Fig.5b. The same as in Fig.3b for $q=1/\tau$.

The results for h=0 and increasing q, and for $q=1/\tau$, h=0.1, h=0.25 are presented in Figs.2-7 and in Figs.8,9, respectively. Notice that for $q \lesssim 0.5$ $\Delta G(x)$ shows sharp peaks in long- and short-wavelentgh limits. They reflect the Van-Hove singularity of density of states of infinite periodic chain [46] given by

$$\rho(x)= \frac{N}{\Pi} \frac{1}{\sqrt{x(4-x)}} . \qquad (15)$$



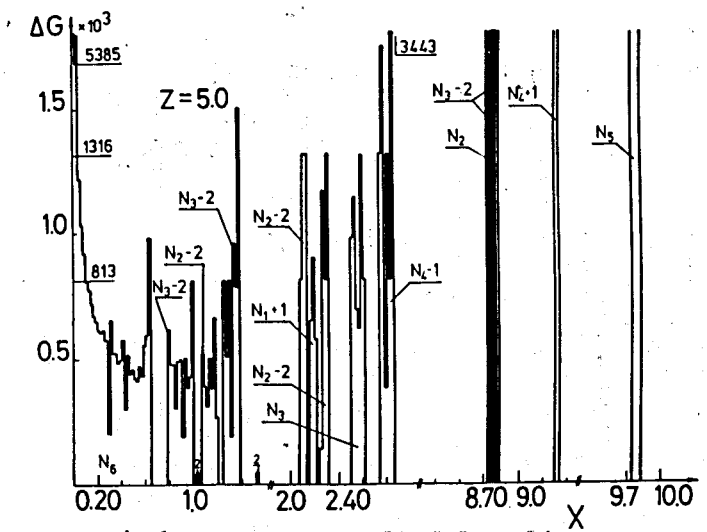


Fig.6a. The same as in Fig.2 for $q=5/\tau$.

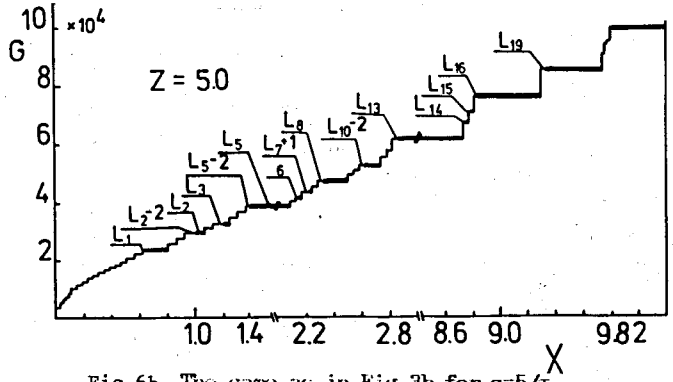


Fig.6b. The same as in Fig.3b for $q=5/\tau$.

The substructure of G(x) and $\Delta G(x)$ in acoustic and optical regions of VS are shown in Figs.10-13 and 14,15, respectively.

In addition, the function $\rho_1(y_1)$ called an average density of states

$$\rho_1(y_1)= \frac{G_1(y_1) - G_1(y_1-\Delta_1)}{N \Delta_1} \qquad (16)$$

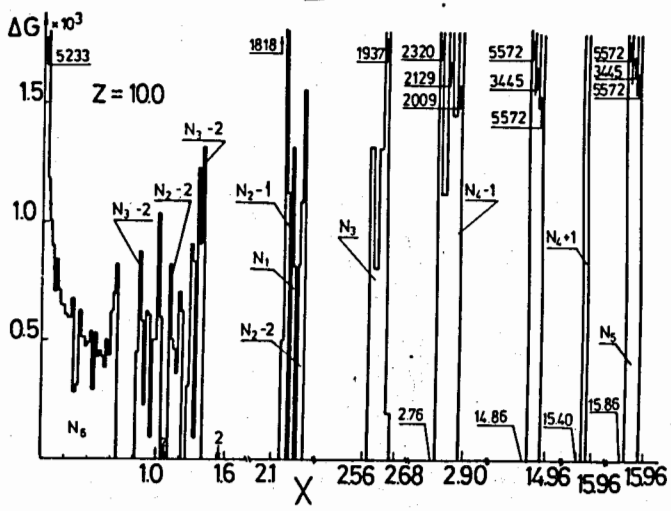


Fig.7a. The same as in Fig.2 for $q=10/\tau$.

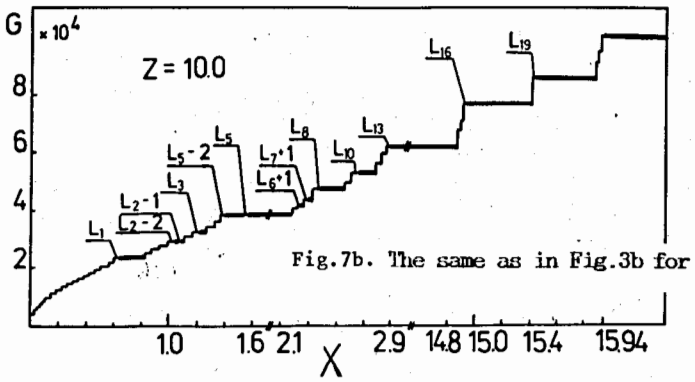


Fig.7b. The same as in Fig.3b for $q=10/\tau$.

is calculated, where $\Delta_1 \le y_1 = \sqrt{x / x_{max}} \le 1$ and $\Delta_1$ is an elementary step of calculation. Notice that $G_1(y_1)$ determines the number of eigenfrequencies of DM obeying the condition $\Omega_i < y_1$.

Dependences of $\rho_1$ on $y_1$ for $q=1.0/\tau$, $h=0$; $q=10/\tau$, $h=0$ and $q=1/\tau$, $h=0.25$ are shown in Figs. 16a, 16b, and 16c, respectively.

The dependence of $\rho_1$ on q and h in acoustic region of VS is presented in Fig.17. Notice that for $q > \exp(2)$ we observe a power dependence of $\rho_1(\Delta_1=1/225)$ on q. The standard analysis of numerical results gives $\rho_1(\Delta_1)=C_1 q^{\gamma}$, where $C=\exp(-0.84)$ and $\gamma=0.46$.



In order to study a hierarchical structure of VS the DM under FEBC is diagonalized by using EISPACK routines ( BANDR and TQLRAT). Computations are performed for the numbers of atoms $F_{15}=610 \le N \le F_{19}=4181$ and various values of model parameters q and h. The results are presented in Fig.18-19.

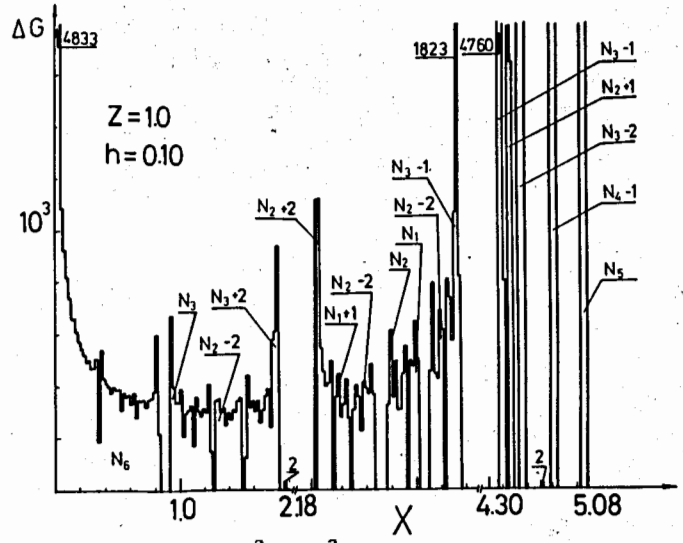


Fig. 8a. ΔG versus $x=\Omega^2=m_o\omega_o^2/k_o$ for $h=0.10$, $q=1/\tau$ and $N=10^5$.

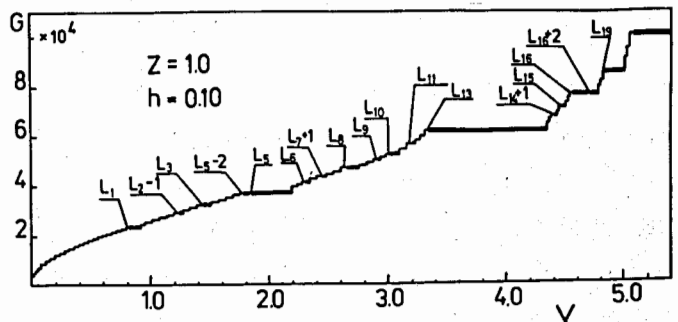


Fig. 8b. G versus $x=\Omega^2=m_o\omega_o^2/k_o$ for $h=0.10$, $q=1/\tau$ and $N=10^5$.

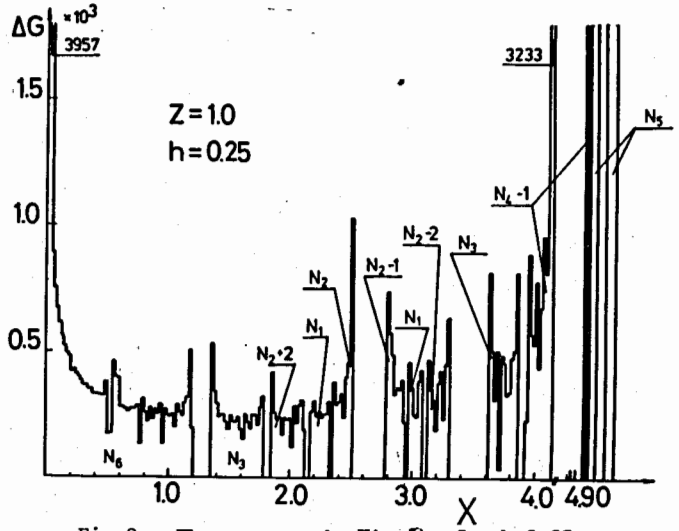


Fig.9a. The same as in Fig.8a for h=0.25.

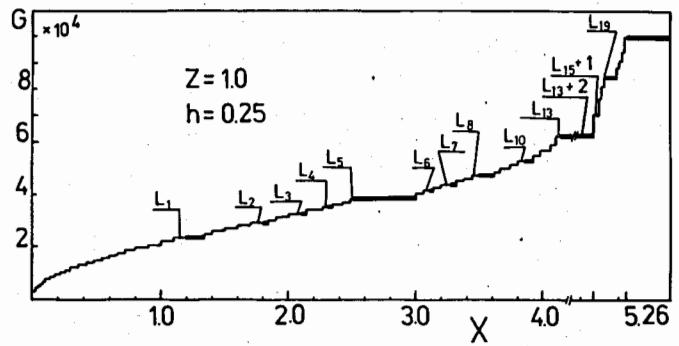


Fig.9b. The same as in Fig.8b for h=0.25.

Moreover, the branching structure of VS is analyzed using the following approach. Let $\delta$ be a real positive number and ( $x_1, x_N$ ) ( ( $\sqrt{x_1}, \sqrt{x_N}$ ) ) denote the vibrational spectrum given in an increasing order of $x_i = \Omega_i^2 / \Omega_{max}^2$ ( $\sqrt{x_i}$) where $\Omega_i$ and $\Omega_{max}$ are the ith and Nth dimensionless eigenfrequency of DM, respectively. Then, we consider $\Omega_i$ and $\Omega_{i+1}$ to be in the same "subband" if $(x_{i+1} - x_i) < \delta$ $((\sqrt{x_{i+1}} - \sqrt{x_i}) < \delta$ ),i.e. $\delta$ denotes here a mini-



Fig.10. G(x) versus x in the acoustic region of VS;q=1.0/r, N=$10^5$; Δ-an elementary step of x; $\Delta_3, \Delta_4, \Delta_5, \Delta_6$ denote the width of gaps occurring near values of G(x) equal to $N_3$=5574, $N_4$=9017, $N_5$= =14589, $N_6$=23607, respectively (see also Table 2).

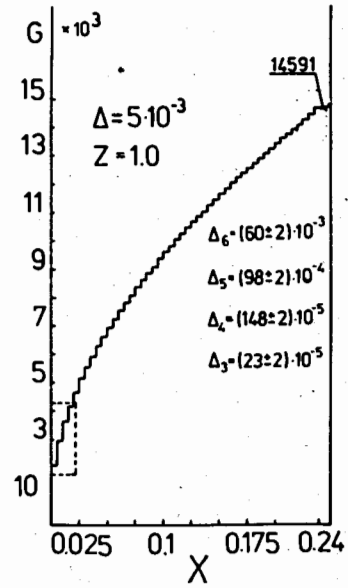


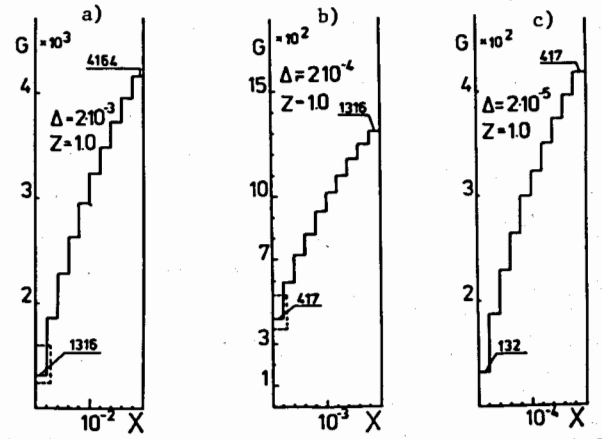


Fig.11. G(x) versus x for x << 1.0,q=1/r, h=0.0 and N = $10^5$; numbers depicted at the bottom and top of each "staircase" give the value of G. (a) $\Delta=2*10^{-3}$, (b) $\Delta=2*10^{-4}$ and (c) $\Delta=2*10^{-5}$ represent G(x) in the regions dashed in Figs.10, 14a and 14b, respectively.

mal width of the distinguishable gap. Using this rule the substructures of VS are determined for decreasing $\delta$ . The results obtained for N=4181, $q=1/\tau$, h=0 are presented in Fig.20.

The fractal dimensions $\bar{d}$ of $(\Omega_1^2,\Omega_N^2)$ and $(\Omega_1,\Omega_N)$ are calculated using Mandelbrots covering method [47] described in Appendix B. In this way we determine $\bar{d}$ within 1% and 10% for $q\simeq 1$ and $q\simeq 10^2$, respectively. The numerical results are shown in Fig.21 and Fig.22.

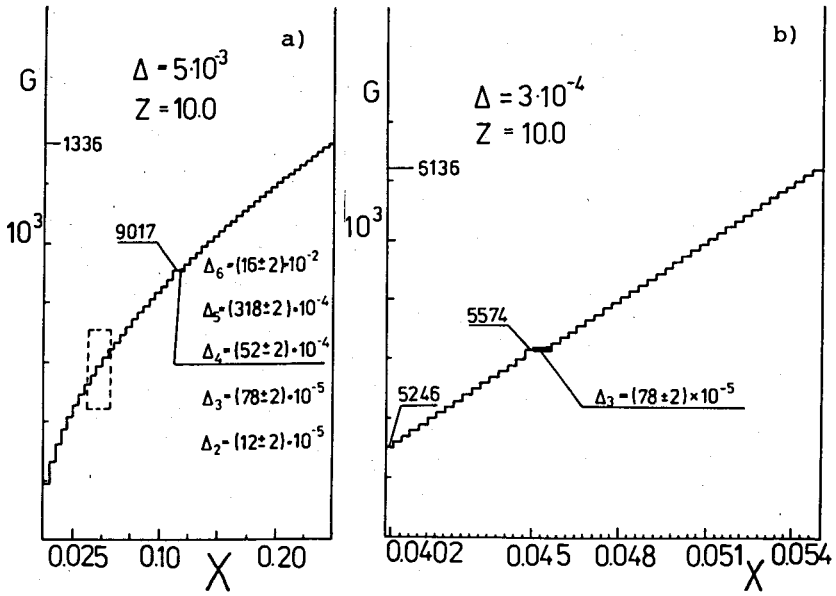


Fig.12. The same as in Fig.1C for $q = 10/\tau$; (a) $\Delta=3*10^{-3}$; $\Delta_2,\Delta_3,\Delta_4,\Delta_5,\Delta_6$, give the width of energetic gaps occurring near values of G equal to $N_2=3445, N_3=5574, N_4=9017, N_5=14589, N_6=23607$, respectively (see also Tab.2); (b) $\Delta=3*10^{-4}$, G(x) versus x in the region dashed in Fig.12a.



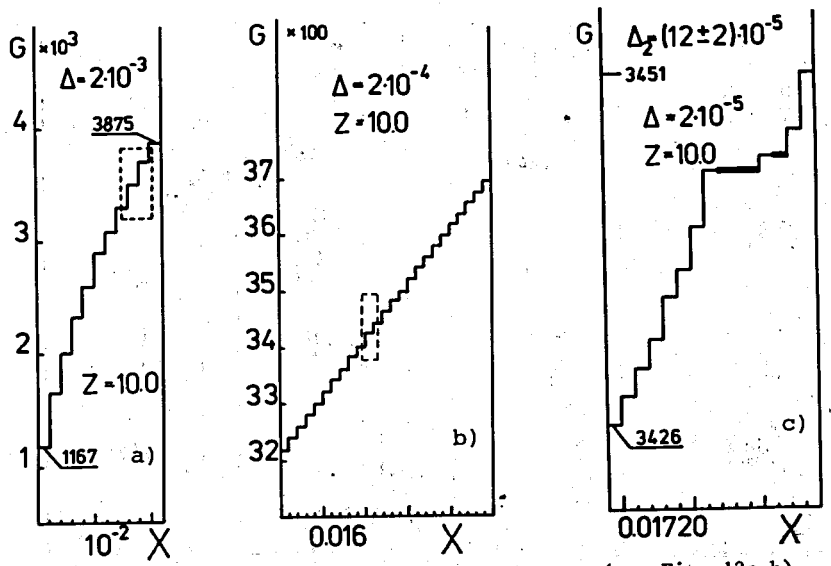


Figs. 13. G(x) as a function of x near $\Delta_2$ gap (see Figs.12a,b) for $x\ll 1, q=10/\tau, h=0, N=10^5$. (a) $\Delta=2*10^{-3}$, (b) $\Delta=2*10^{-4}$, and (c) $\Delta=2*10^{-5}$ represent G(x) in the regions dashed in Figs.13a and 13b, respectively.

## 5. Conclusions

From the results presented in the previous section one can draw the following conclusions.

1. The Cantor-set-like character of VS manifests itself in the optical region very well (cf. Figs.4-9, 14-16, 18,19) and almost disappears in the long-wavelength limit ( cf. Figs. 3-13,16, 18) [22,32,35].

2. The width $\Delta_g$ of the gap is an increasing function of q. This implies that peaks of $\Delta G(x)$ become in general narrower and higher as q increases (cf. Figs.3-7).

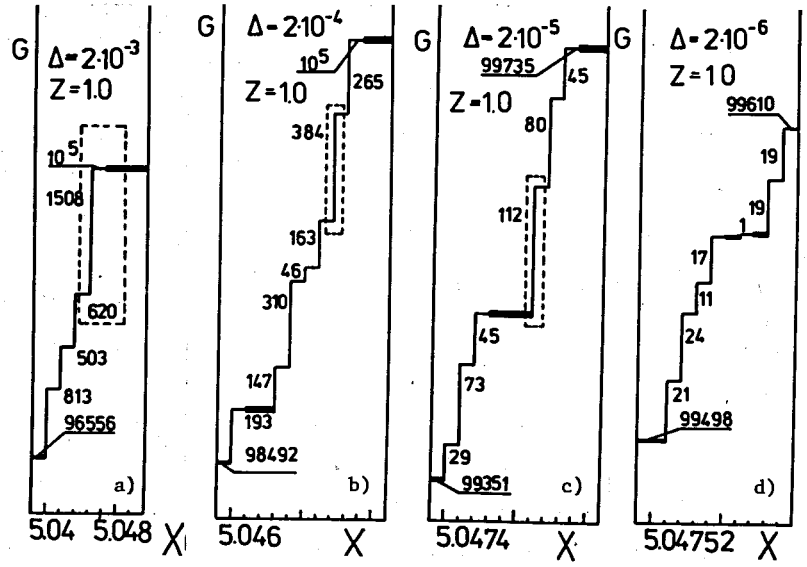


Fig. 14. G(x) versus x in the optical region of VS; $q=1/\tau$, $h=0.0$, $N=10^5$. The numbers depicted inside the figures give the values of $G(x)-G(x-\Delta)$. (a) $\Delta=2*10^{-3}$, (b) $\Delta=2*10^{-4}$, (c) $\Delta=2*10^{-5}$ and (d) $\Delta=2*10^{-6}$ represent G(x) in the regions dashed in Figs. 14a, 14 and 14c, respectively.

3. For given q and h the width of $\Delta_g$ depends on its position in the phonon spectrum and tends to zero in the short- and long-wavelentgh limits (cf. Figs. 3b-9b, 13-16) [32,35].

4. If one neglects the gaps whose widths are less than a given number $\Delta_g > 0$, then VS are "band-like" and near the edges of each subband $\Delta G(x)$ and $\rho_1(y_1)$ exhibit Van Hove singularities (cf. Fig. 3a-9a) [32].

5. In the acoustic region $x \leq 0.1$ phonon spectra have the quasi-continuous character (cf. Figs. 3-13). Eigenfrequencies of DM for



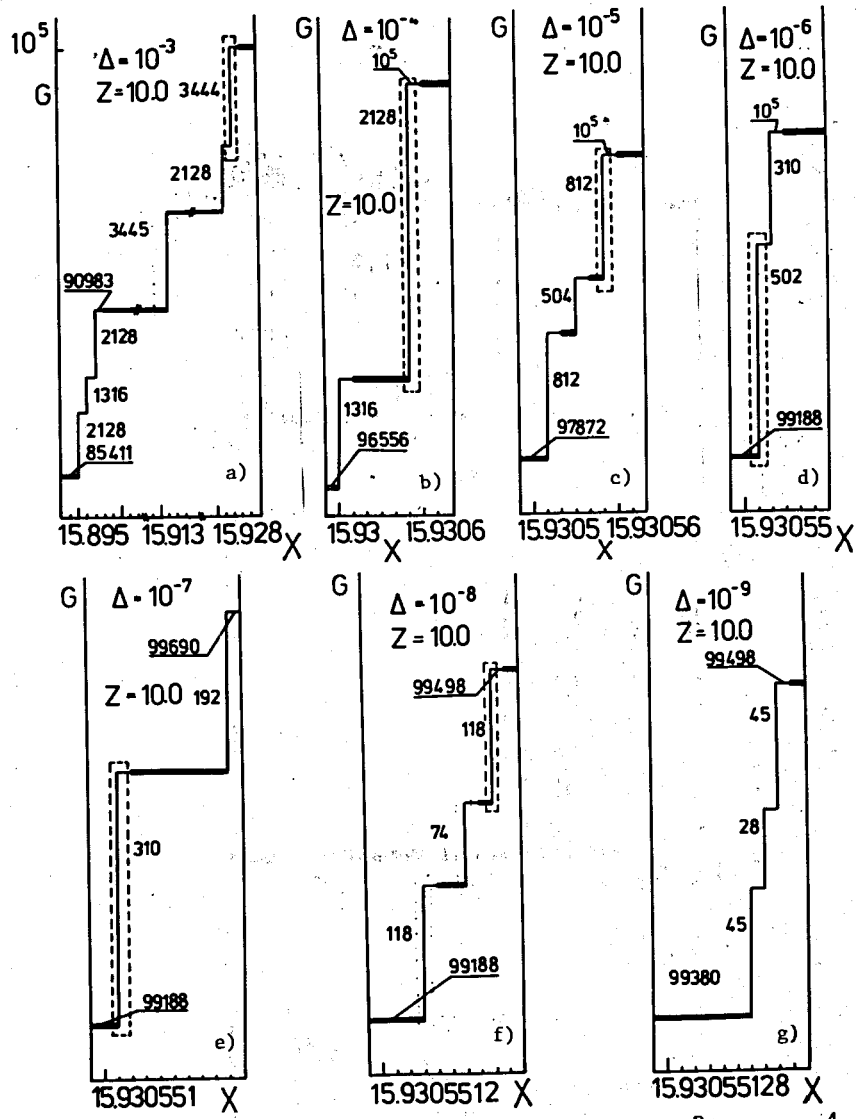


Figs. 15. The same as in Fig. 14 for $q=10/\tau$. (a) $\Delta=10^{-3}$, (b) $\Delta=10^{-4}$, (c) $\Delta=10^{-5}$, (d) $\Delta=10^{-6}$, (e) $\Delta=10^{-7}$, (f) $\Delta=10^{-8}$ and (g) $\Delta=10^{-9}$ show dependences of G on x in the regions dashed in Figs. 15a-15f, respectively.

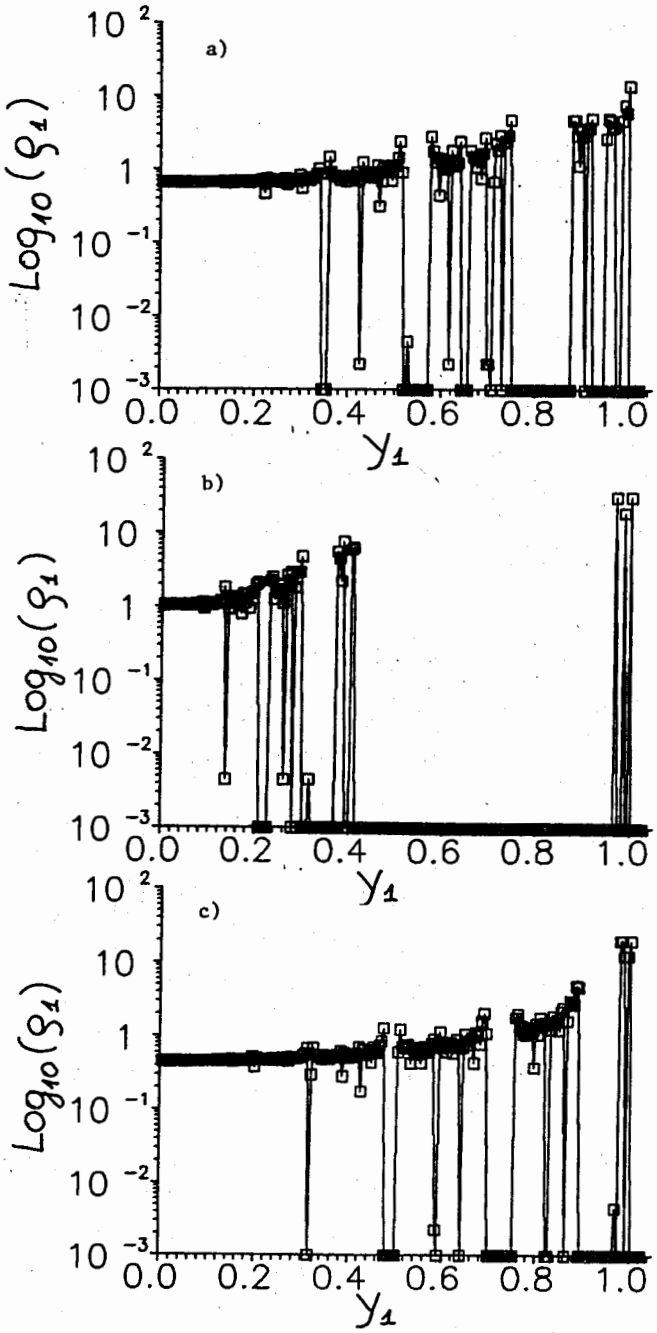




Figs.16. $Log_{10}(\rho_1)$ versus $y_1$; step of calculation $\Delta_1=1/225$, $N=10^{+5}$; (a) $z=1/\tau$, $h=0$; (b) $q=10/\tau$, $h=0$; (c) $q=1/\tau$, $h=0.25$; $\rho_1=0$ are depicted as $\rho_1=10^{-3}$. Values of $\rho_1$ having $\log_{10}(\rho_1)$ less than $10^{-2}$ correspond to isolated states in the gaps.

$1 \le i \le [\, N / \tau^5 \,]$ are given within 3% by

$$\Omega_i = 2\,\Gamma_i(q,h)\,\sin\left[\frac{(i-1)\Pi}{2N}\right] \quad 2\,\Gamma_2(q,h)\,\sin\left[\frac{(i-1)\Pi}{2N}\right], \qquad (17)$$

where $\Gamma_i = \Omega_i(q,h)/\Omega_i(0,0)$. Dependences of $\Gamma_2$ on q at h =0 and on h for fixed q are presented in Figs. 23a-c and 23d, respectively. Notice that $\Gamma_2$ shows a linear dependence $\Gamma_2(q)=1+0.177*q$ on q for $q \le 0.1$ (cf. Figs.23a,b) and a saturation effect for large q ( cf. Fig.23c). Moreover, $\Gamma_2$ increases almost linearly with h (cf. Fig. 23d) and the fit of linear function to numerical results gives $\Gamma_2 = 1.372*h + 1.112$ and $\Gamma_2 = 1.330*h + 1.247$ for $q=1/\tau$ and $q = 10/\tau$, respectively. Therefore, one observes the following facts: (1) dependence of G on x has the form $G(x)=G_0(q,h)\sqrt{x}$, where $G_0(q,h)$ denotes quantity depending on model parameters (cf.Figs.10,12a); (2) histograms $\Delta G(x)$ show Van Hove singularity at $x \to 0$, i.e., $\Delta G(x) = \Delta G_0(q,h) / \sqrt{x}$ ( cf. Figs. 3a-9a ); (3) the average density of states $\rho_1(y_1)$ does not depend on $y_1$ (cf. Fig.16)

$$\lim_{y_1 \to 0} \rho_1(y_1) = C_1(q, h), \qquad (18)$$

where C is a constant at given q and h (cf. Fig.17)

Notice that the width of the acoustic (quasicontinuous) region of VS is a decreasing function of q ( cf. Figs.3-9,16 ).

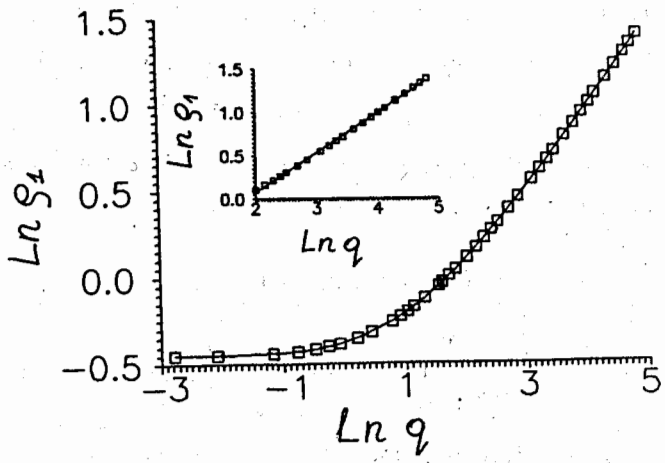


Fig.17a. Ln($\rho_1(\Delta_1)$) versus ln(q); inset shows the linear dependence of ln($\rho_1$) on ln(q) observed for large q . The best fit for q > exp(2) gives ln($\rho_1$) = 0.46 ln(q) - 0.84.

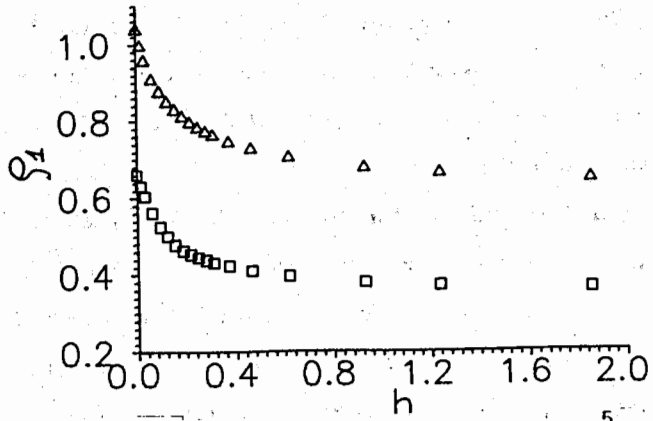


Fig. 17b. $\rho_1$ as a function of h, $z=1/\tau$, $N=10^5$.

6. Vibrational spectra of harmonic models of 1D FQC's are self-similar (cf. Figs.19-20) [22,26,32,38]. In the following hierarchies each subband is branching into subbands according to the rule [35]

$$N_i = N_{i-1} + N_{i-2} = N_{i-2} + N_{i-3} + N_{i-2}\,, \qquad (17)$$



Table 1. Values of $L_i$ used in Figs.3b-9b.

| | |
|---|---|
| $L_1$ = 23607 | $L_{12}$ = 58361 |
| $L_2$ = 29181 | $L_{13}$ = 61804 |
| $L_3$ = 32624 | $L_{14}$ = 67376 |
| $L_4$ = 34754 | $L_{15}$ = 70821 |
| $L_5$ = 38198 | $L_{16}$ = 76393 |
| $L_6$ = 41641 | $L_{17}$ = 79838 |
| $L_7$ = 43770 | $L_{18}$ = 81966 |
| $L_8$ = 47214 | $L_{19}$ = 85411 |
| $L_9$ = 50659 | $L_{20}$ = 90983 |
| $L_{10}$ = 52788 | $L_{21}$ = 94428 |
| $L_{11}$ = 56231 | |

Table 2. Values of $N_i$ used in Figs.3a-9a. In the second column the numbers $[N/\tau^j] \simeq N_i$ are given (see also Fig.24 where $[N/\tau^j]$ correspond to $N_{100\ldots}$ of (j+1)th level)

| | |
|---|---|
| $N_0$= 1315 | ; $[N/\tau^0]$ |
| $N_1$= 2129 | ; $[N/\tau^8]$ |
| $N_2$= 3445 | ; $[N/\tau^7]$ |
| $N_3$= 5574 | ; $[N/\tau^6]$ |
| $N_4$= 9017 | ; $[N/\tau^5]$ |
| $N_5$= 14589 | ; $[N/\tau^4]$ |
| $N_6$= 23607 | ; $[N/\tau^3]$ |
| $N_7$= 38198 | ; $[N/\tau^2]$ |
| $N_8$= 61803 | ; $[N/\tau]$ |

where $N_i$ , $N_{i-1}=N_i/\tau$ and $N_{i-2}=(1-1/\tau)N_i$ denote number of eigenstates in subbands. The hierarchical structure of VS is shown schematically in Fig.24, where $\delta_i$ and $N_{k_1\ldots k_i}$ denote a minimal width of distinguishable gap and numbers of eigenfrequencies in subband on the i-th level, respectively; $k_i = 0$ , 1 and the number $N_{k_1,\ldots,k_i}$ of the i-th level is connected with $N_{k_1\ldots k_{i-1}}$ by

$$N_{k_1,\ldots,k_i} = k_i\, N_{k_1,\ldots,k_i}/\tau + (1-k_i)\, N_{k_1,\ldots,k_i}(1-1/\tau) = N_{k_1,\ldots,1} + N_{k_1,\ldots,0}. \qquad (18)$$

The described Cantor-set-like structure of VS is independent of model parameters and comes from the quasiperiodicity of the Fibonacci chain.

7. The fractal dimension $\bar{d}$ of phonon spectra ( $\Omega_1^2$, $\Omega_N^2$ ) shows a power-law decay if POQ increases. The best fit of the power function $q^{\alpha}$ to the calculated results at $q \geq 0.5/\tau$ gives

$$\bar{d} = C * q^{\alpha}, \qquad (19)$$

where $\alpha=-(0.11 + 0.02)$ and $C = 0.82 + 0.03$. Dependence of fractal dimension $\bar{d}_1$ of phonon spectra $(\Omega_1, \Omega_N)$ on q has a similar form

$$\bar{d}_1 = C_1 * q^{\alpha_1}, \qquad (20)$$

where $\alpha_1=-(0.05 + 0.01)$ and $C_1 = 0.91 + 0.02$. Notice that $\bar{d} \simeq \bar{d}_1^2$

Fig.18a-f. Phonon spectrum of the harmonic model of lattice dynamics of 1D FQ for $N=F_{15}=610$, $q=1/\tau$ and increasing h. Square of eigenfrequency versus mode number: (a) h=0.15; (b) h=0.25 ; (c) h=0.35 ; (d)=0.45 ; (e) h=0.55; (f) h=0.55 for $N \geq F_{13} = 233$.



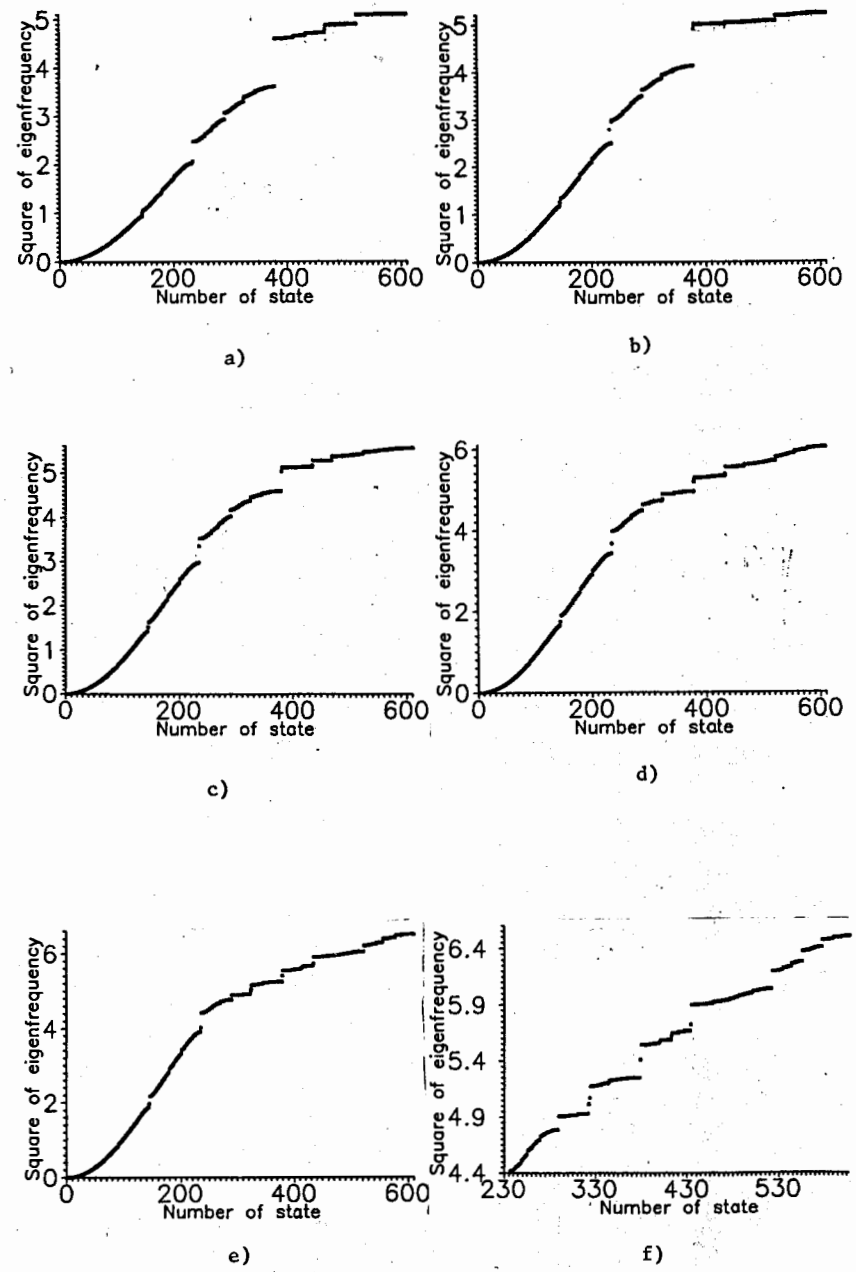

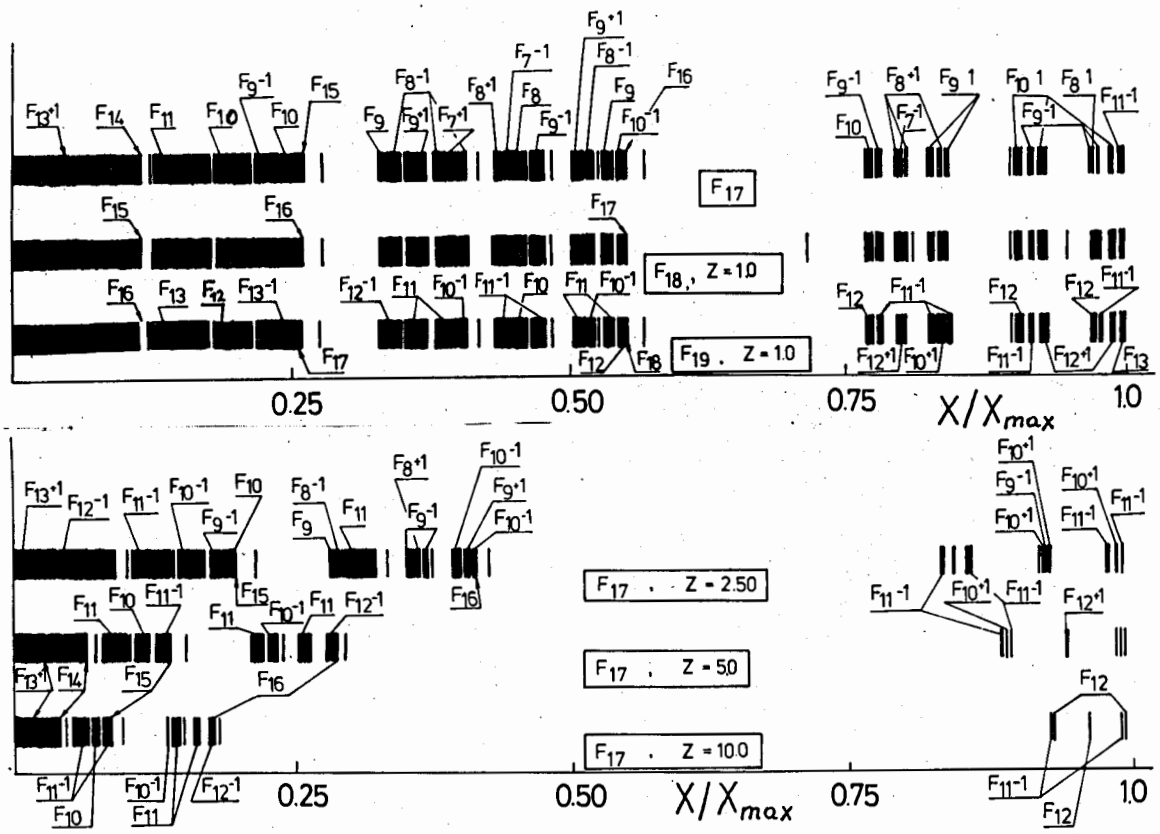




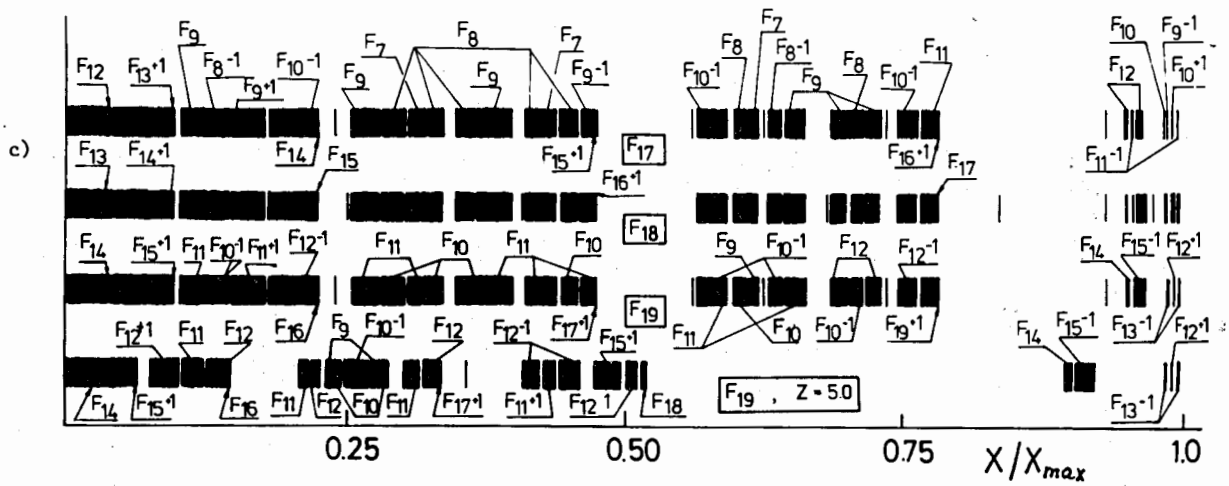




Fig.19a-c. The substructure of the vibrational spectrum of 1D FQC's; on the abscissa axis the values of $x/x_{max}=\Omega^2/\Omega^2_{max}$ are given. (a) VS for a growing number of atoms in the chain $N=F_{17}=1597$, $N=F_{18}=2584$, $N=F_{19}=4181$; $q=1/r$, $h=0$; the depicted Fibbonacci numbers $F_i$ give the number of state in distinguishable (at used scale) subbands. (b) The same as in (a) for increasing $q=z/r$; $N=F_{17}$. (c) The same as in (a); $h=0.25$, $q=1/r$, $N=F_{17}$, $F_{18}$ or $F_{19}$; at the bottom of figure the spectrum for $q=5/r$, $h=0.25$ and $N=F_{19}$ is presented.

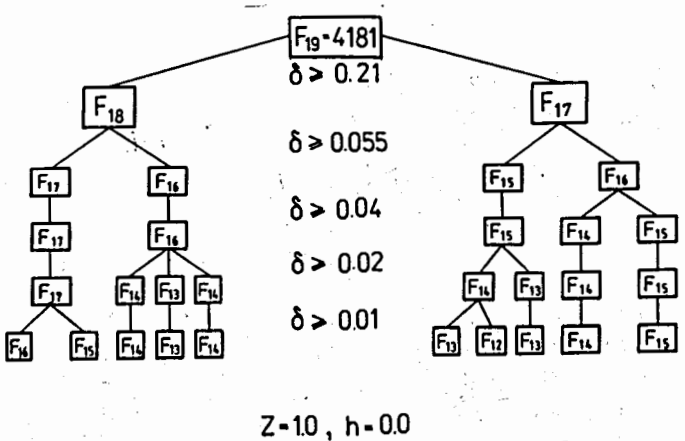


Fig. 20. The hierarchical structure of the vibrational spectrum obtained for decreasing $\delta$; $q=1/\tau$, $h=0$, $N=F_{19}=4181$.

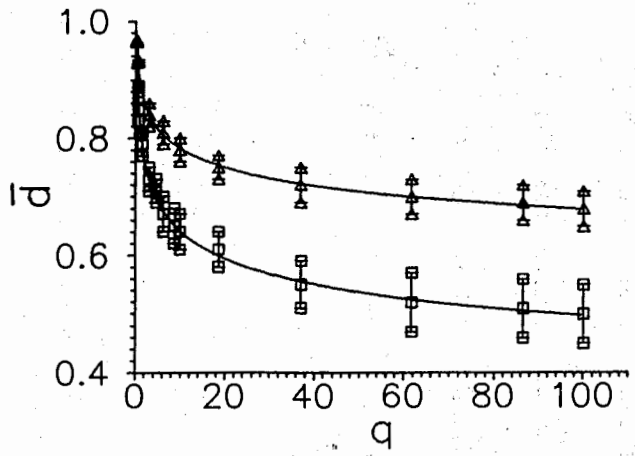


Fig. 21. The fractal dimension $\bar{d}$ versus q for $N=F_{19}=4181$. Triangles ( $\nabla$ ) and squares ( $\square$ ) represent values of $\bar{d}$ corresponding to ( $\Omega_{min}$,$\Omega_{max}$) and ( $\Omega^2_{min}$,$\Omega^2_{max}$), respectively. The solid lines represent the power functions $\bar{d}_1 = 0.91*q^{-0.05}$ and $\bar{d} = 0.82*q^{-0.11}$ obtained by fitting the function $q^{\alpha}$ to the calculated results for $q \geq 0.5/\tau$.



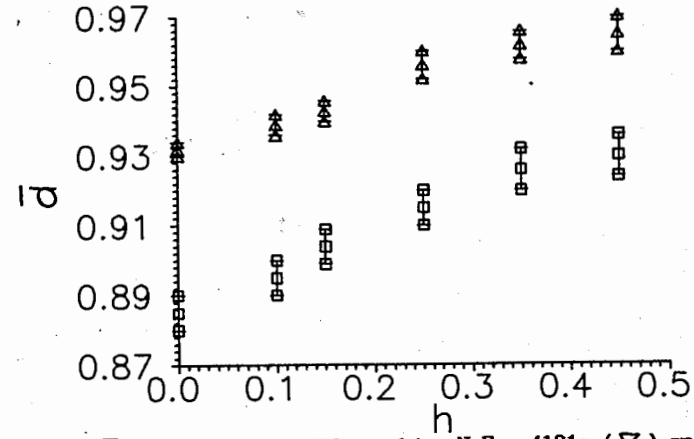


Fig. 22. $\bar{d}$ as a function of h; $q=1/\tau$, $N=F_{19}=4181$; ( $\nabla$ ) and ( $\square$ ) correspond to ( $\Omega_{min}$,$\Omega_{max}$) and ( $\Omega^2_{min}$,$\Omega^2_{max}$), respectively.

8. VS exhibit characteristic tendencies as the degree of next-nearest-neighbour interaction increases. In particular:

- spectra show a general drift towards higher frequencies (cf. Figs.8,9,18);
- peaks of $\Delta G(x)$ become more pronounced in the optical region and density of states in the acoustic region decreases ( compare Fig.5 and Figs.8,9);
- the width of gaps decreases (compare Fig.5 and Figs.8,9; cf. Fig.18);
- the fractal dimension enlarges (cf. Fig.22).

9. There exist eigenstates $\Omega_g$ inside some gaps ( cf. Figs.3-9,

16,18,19). We have verified that eigenvectors of DM corresponding to $\Omega_s$ have the localized character and are surface states [ 28, 48].

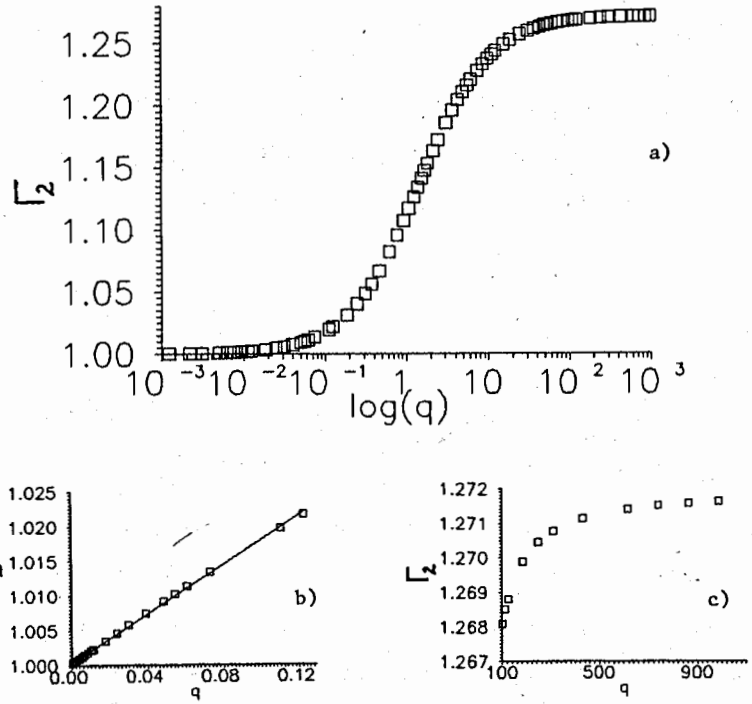


Fig. 23a-c. Dependences of $\Gamma_2(q,h=0) = \Omega_2(q,h=0)/\Omega_2(0,0)$ on q, $F_{17}$ =1597; (a) $\Gamma_2(q,h=0)$ versus log(q); (b) linear dependence $\Gamma_2(q,h=0)=1+0.177*q$ observed for $q \leq 0.10$; (c) saturation effect in dependence of $\Gamma_2(q,h=0)$ on q.



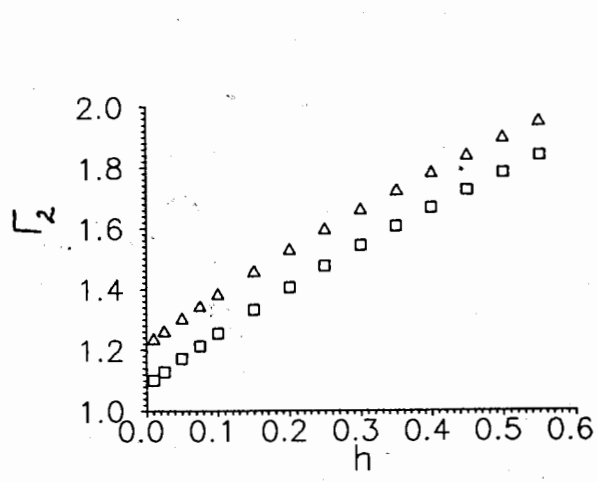


Fig.23d. $\Gamma_2$ ( q, h ) = $\Omega_2$ ( q , h )/ $\Omega_2$( 0 , 0 ) versus h, $N=F_{17}$; ($\Delta$) q = $10/\tau$ = 0.618....; ($\square$) q = 1 / $\tau$ = 6.180.....

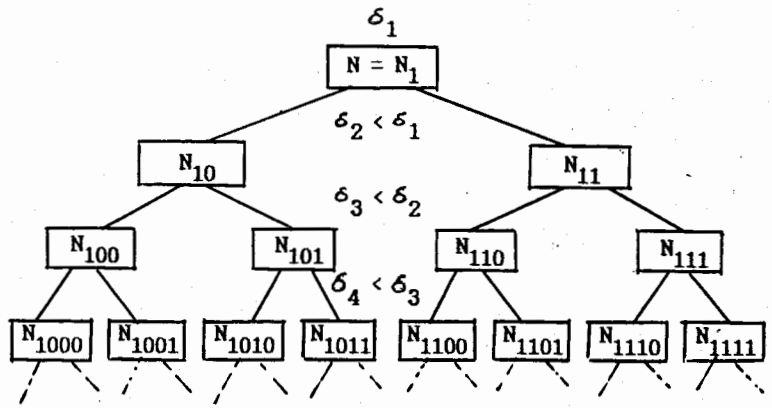


Fig.24. Schematic representation of the hierarchical structure of VS obtained for decreasing $\delta$. N is an initial number of states in VS; $\delta_i$ and $N_{k_1,\ldots,k_i}$ denote a minimal width of distinguishable gap and number of eigenstates in the subband on the ith hierarchical level, respectively.

## 6. Summary

The properties of vibrational spectra of the harmonic model describing lattice dynamics of the Fibonacci-type chain of atom have been studied numerically. Computer simulations have been done under free end boundary conditions. The vibrational spectra show properties of both the ideal (periodic) and disorder ( glassy) chain. On the one hand, in the acoustic limit they have a quasicontinuos character and exhibit bandlike properties if small gaps are neglected. On the other hand, in the optical region they show a Cantor-set-like substructure. These general properties of VS are independet of model parameters $q > 0$ , h and are a consequence of quasiperiodic long-range positional order of Fibonacci chain [ 3 - 5 ].

IDOS, its histograms and average density of states have been calculated in the wide range of model parameters. Main tendencies in dependences of G, $\Delta G$ and $\rho_1$ on q and h have been determined.

Fractal dimension $\bar{d}$ of VS has been calculated for $N=F_{19}=4181$, $h = 0$ and increasing q; $\bar{d}$ shows a power-law dependence on q for $q \leq 0.1$. Moreover, the performed calculations of $\bar{d}$ for $N = F_{19} = 4181$, $q=1/\tau$ and $h\neq 0$ indicated that $\bar{d}$ increases with h.

Finally, we point out that in the acoustic region the phonon spectrum of the studied harmonic model behaves almost identically as for the ideal periodic chain. Therefore, we can expect that the thermodynamic properties of 1D FQC's and ideal chains should not differ essentially. Our investigations of the temperature dependence of heat capacity [ 49,50 ] confirm this presumption .



Some further information about the structure of VS can be obtained from the properties of eigenvectors of DM. This will be the subject of a separate paper [48].

Acknowledgments

I would like to thank Prof. N.M. Plakida for valuable remarks and comments. I am grateful to Dr. J.Malek who helped me in preparation of numerical programs. Computations have been done at the Laboratory of Computing Techniques and Automation of Joint Institute for Nuclear Research.

## Appendix A

The mathematical properties of the infinite BQS's given by (4) and (5) are as follows:

A1. In BQS's, (4) and (5), one of the two constituents, i.e., $k_o$ ( 1 + q ) and $g_o$ in the case of (4) and (5), respectively, always appears isolated. The other elements occur in a string of consecutive elements .

A2. The BQS, (4), is a $k_o$-dominant one and contains strings of consecutive $k_o$ of sizes 1 or 2 only, separated by isolated $k_o$( 1 + q ) .

A3. The BQS, (5), is a $g_o$ ( 1 + q )-dominant one and the sizes of the strings of consecutive elements $g_o$ ( 1 + q ) are equal to 2 or 4 .

A4. Sequence (5) can be obtained from the sequence (4) by replacing $k_o$ by $\{ g_o(1+q), g_o(1+q) \}$ and $k_o(1+q)$ by $g_o$, i.e. BQS $\{ g_{l,l+2} \}$ is a successor of the BQS $\{k_{l,l+1}\}$ [43,44].

A5. The ratio of the number of $k_o$ and $k_o(1+q)$ or $g_o(1+q)$ and $g_o$ in the infinite sequences (4) and (5), respectively, are given by

$$\frac{N_{k_o}}{N_{k_o(1+q)}} = \tau \quad \text{and} \quad \frac{N_{g_o(1+q)}}{N_{g_o}} = 2\tau .$$

A6. The BQS (4) takes its $k_o$ and $k_o(1+q)$ values on the sets

$$C_{k_o} : \{ l \mid l=[m\tau] , m \in N \}$$

and

$$C_{k_o(1+p)} : \{ l \mid l=[ m \frac{\tau}{\tau-1} ], m \in N \} ,$$

respectively.

A7. The quasiperiodic sequence (5) takes its $g_o$ and $g_o(1+q)$ values on the sets

$$C_{g_o} : C_1' \cap C_1$$

$$C_{g_o(1+q)} : C_1' \cup C_1 - C_2 , \text{ respectively, where}$$

$$C_1' : \{ l' \mid l' = [ m\tau ] - 1 , m \geq 2 \} \text{ and}$$

$$C_2 : \{ n' \mid n' = [n \frac{\tau}{\tau - 1} ] - 1 , n \geq 2 \}.$$

Appendix B

We explain briefly the used method of calculation of fractal dimension $\bar{d}$ .



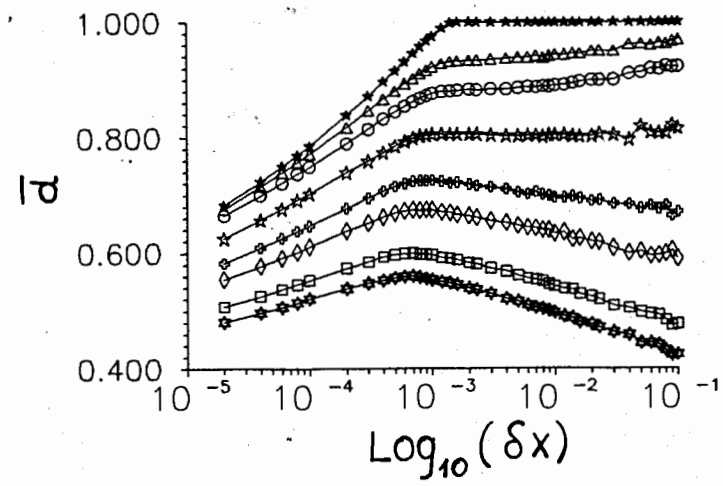


Fig.C1. Fractal dimension $\bar{d}$ of( $\Omega_1^2$ ,$\Omega_N^2$ ) versus $\delta x$ for increasing $q=z/\tau$ ; (★) z=0; (△) z=0.5; (○) z=1; (☆) z=2.5; (✠) z=7.5; (◊) z=16; (□) z=60; (✡) z=140; N=4181, $M_2$=1; solid lines are depicted for eyes.

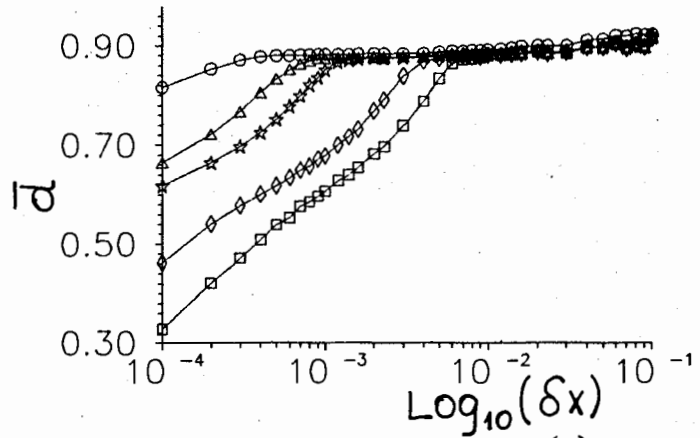


Fig.C2. The same as in Fig.C1 for various $M_2$: (○) $M_2=F_1=1$; (△) $M_2=F_2=2$; (☆) $M_2=F_3=3$; (◊) $M_2=F_5=8$; (□) $M_2=F_6=13$; $N=F_{19}=4181$, z=1,h=0; solid lines are depicted for eyes.

Let $\delta x$ ($\delta y_1$) be the real positive number. We cover the spectrum ( $\Omega_1^2$, $\Omega_N^2$ ), ( ( $\Omega_1$, $\Omega_N$ ) ) of DM with the segments whose lengths are $\delta x$ ($\delta y_1$). Let $N_i(\delta x)$ ( $N_i'(\delta y_1)$) denote the number of eigenstates inside of the i-th segment. We determine the number $M_1$ of segments fulfilling the condition $N_i(\delta x) \geq M_2$ ( $N_i(\delta y_1) \geq M_2$ ), where $M_2$ is a given natural number. Then, according to [47]

$$\bar{d} = \frac{\mathrm{Ln}\,(M_1)}{\mathrm{Ln}\,(M_0)},$$

where $M_0$ is equal to [ $x_{max} / \delta x$ ] ( [ $\sqrt{x_{max}} / \delta y_1$] ); [z] denotes the integral part of z.

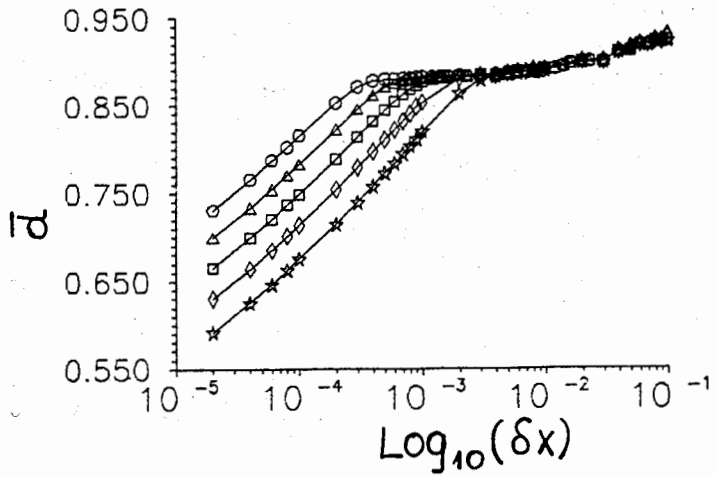


Fig.C3. The same as in Fig.C1 for for increasing N, (○) $N=F_{19}=10946$; (△) $N=F_{18}=6564$; (□) $N=F_{17}=4181$; (◇) $N=F_{16}=2581$; (☆) $N=F_{15}=1597$; z=1, solid lines are depicted for eyes.



We have investigated dependences of $\bar{d}$ on the number N of atoms in the chain and the magnitudes of $\delta x$ and $M_2$. The numerical results show (cf. Figs.C1-C3) the existence of a plateau ( with the width depending on N, $\delta x$ and $M_2$) in dependences of $\bar{d}$ on $\delta x$ which allow us to determine $\bar{d}$. The results presented in Sec.4 have been obtained for $N=F_{19}=4181$ and $M_2=1,3,8$.

References


1. D.S.Schechtman, I.Blech, D.Gratias, J.W.Cahn, Phys. Rev. Lett. 53,1951 (1984)
2. Workshop on Aperiodic Crystals, Eds. L.Michel and D.Gratias, J. Physique Colloq. 47, C3 (1986)
3. D.Levine, P.J.Steinhardt, Phys. Rev. Lett. 53, 2477 (1984)
4. D.Levine, P.J.Steinhardt, Phys. Rev. B34,596 (1986)
5. J.E.S.Socolar, P.J.Steinhardt, ibid., B34,617 (1986)
6. J.E.S.Socolar, T.C.Lubensky, P.J.Steinhardt, ibid.,B34, 3345 (1986)
7. C.L.Henley,ibid.,B34,797 (1986)
8. P.De, R.A.Pelcovits, ibid., B35, 8609 (1987)
9. Y.Shen, W.Dmowski, T.Egami, S.J.Poon, G.J.Shiflet, ibid.,B37, 1146(1988).
10. A.Yamamoto, K.Haraga, ibid., B37, 6207 (1988)
11. D.S.Rokhsar,N.D.Mermin, D.C.Wright, ibid. B37,5487 (1988)
12. J.W.Cahn, D.Gratias, B.Mozer, J. Phys. France 49, 1225 (1988)
13. J.W.Cahn, D.Gratias, B.Mozer, Phys.Rev. B38, 1638 (1988)
14. D.Gratias, J.W.Cahn, B.Mozer, ibid. B38, 1643 (1988)

15.H.B.Elswijk, J.Th.De Hosson, S.Smaalen, J.L.De Boer, ibid., B38, 1681 (1988)

16.R.Riklund, M.Severin, Y.Liu, Inter. J. Mod. Phys. B1, 121 (1987)

17.Z.Cheng, R.Savit, R.Merlin, Phys. Rev. B37, 4375 (1988)

18.S.Aubry, C.Godreche, J.M.Luck, Europhys. Lett. 4,639 (1987)

19.C.Godreche, J.M.Luck, F.Vallet, J. Phys. A20, 4483 (1987)

20.L.S.Levitov, Europhys. Lett. 6 , 517 (1988)

21.R.V.Galiulin, Kristallografiya 25, 901 (1980)

22.M.Kohmoto, J.R.Banavar, Phys. Rev. B34,563 (1986)

23.M.Kohmoto, B.Sutherland, ibid., B34, 3849 (1986)

24.B.Sutherland, ibid., B34, 3904 (1986)

25.M.Kohmoto, ibid., B34, 5043 (1986)

26.M.Kohmoto, B.Sutherland, Ch.Tang, ibid., B35, 1020 (1987)

27.Y.Liu, R.Riklund, ibid., B35, 6034 (1987)

28.M.Arai,T.Tokihiro,T.Fujiwara, J.Phys.Soc.Jap., 56,1642 (1987)

29.F.Aguilera-Granja,F.Mejia-Lira,J.L.Moran-Lopez,R.G.Barrera, Phys.Rev.,B36,7342 (1987)

30.T.Fujiwara, M.Arai, T.Tohikiro, M.Kohmoto, ibid,. B37, 2797 (1988)

31.H.Tsunetsugu,K.Ueda, ibid.,B38,10109 (1988)

32.J.P.Lu, T.Odagaki, J.L.Birman, ibid., B33, 4809 (1986).

33.J.M.Luck, D.Petritis, J. Stat. Phys. 42, 289 (1986)

34.L.Chen, G.Hu, R.Tao, Phys. Lett. 117A,120 (1986)

35.F.Nori, J.P.Rodriguez,Phys. Rev. B34, 2207 (1986)

36.S.E.Burkov, J. Stat. Phys. 47, 409 (1987)

37.B.Chen, Ch.Gong, Z. Phys. B69, 103 (1987)



38.M.C.Valsakumar, G.Ananthakrishna, J. Phys. C20, 9 (1987)

39.D.Wurtz, T.Schneider, A.Politi, Phys. Lett. 129A, 88 (1988)

40.H.De Raedt, T.Schneider, Z. Phys. B71, 287 (1988)

41.J.P.Lu, J.L.Birman, Phys.Rev. B38, 8067 (1988)

42.F.Dyson, Phys.Rev. 92, 1331 (1953)

43.I.Aviram, J. Phys. A19, 3299 (1986)

44.I.Aviram, ibid., A20, 1025 (1987)

45.P.Dean, Rev. Mod. Phys. 44, 127 (1972)

46.N.W.Ashcroft, N.D.Mermin, Solid State Physics, Holt,Rinehart and Winston, New York 1976; Chap.23.

47.B.B.Mandelbrot, The fractal Geometry of Nature, W.H. Freeman Company, New York , 1983

48.W.Salejda (in preparation)

49.W.Salejda, Commun. Joint Ins. Nuc. Res.,E17-88-880 (1988)

50.W.Salejda, Preprint Joint Ins. Nuc. Res.,E17-88-881 (1988) /accepted for publication in International Journal of Modern Physics B, 1989 /

Received by Publishing Department
on April 21, 1989.